administered by the American Chemical Society. Appreciation is expressed to Patricia Klahn-Coble for assistance with the NMR measurements, to Jeffrey Petersen for helpful discussion, and to Robert R. Burch, Jr., who made the first compounds of this type.

Registry No. $1^-Et_4N^+$, 89231-95-8; $1^-Ph_4P^+$, 89232-02-0; $2^-Et_4N_+$, 89231-97-0; $2^-Ph_4P^+$, 89232-03-1; $3^-Et_4N^+$, 89231-99-2; $4^-Et_4N^+$, 89232-01-9; $4^-Ph_4P^+$, 89255-66-3; $(\mu\text{-}Ph_2PCH_2PPh_2)(\mu\text{-}Ph_2P(CH_2)_2PPh_2)Mo_2(CO)_8$, 89232-04-2; $(\mu\text{-}Ph_2P(CH_2)_2PPh_2)_2Mo_2(CO)_8$, 89232-05-3; $(\mu\text{-}Ph_2P(CH_2)_2PPh_2)(\mu\text{-}Ph_2As(CH_2)_2AsPh_2)Mo_2(CO)_8$, 89232-06-4; $(\mu\text{-}Ph_2P(CH_2)_2PPh_2)[Mo(CO)_4(C{\equiv}N)C(CH_3)_3]_2$, 89232-07-5; $Et_4N^+\mu\text{-}HMo_2(CO)_{10}^-$, 12082-98-3; $Ph_4P^+\mu\text{-}HMo_2(CO)_{10}^-$, 89255-65-2; $H^+PF_6^-$, 16940-81-1; CF_3COOH, 76-05-1.

Supplementary Material Available: Comprehensive listings of bond lengths and angles for $Ph_4P^+\mathbf{1}^-$, Table S1, and $Et_4N^+\mathbf{4}^-$, Table S2; observed and calculated structure factors, Tables S3 and S4; and anisotropic thermal parameters, Tables S5 and S6, for both structures (34 pages). Ordering information is given on any current masthead page.

Partial Electron Delocalization in a Mixed-Valence Trinuclear Iron(III)–Iron(II) Complex[1]

Roderick D. Cannon,*[2a] Ladda Montri,[2a] David B. Brown,[2b,c] Kerry M. Marshall,[2b] and C. Michael Elliott[2d]

Contribution from the School of Chemical Sciences, University of East Anglia, Norwich NR4 7TJ, England, Department of Chemistry, University of Vermont, Burlington, Vermont 05405, and Department of Chemistry, Colorado State University, Fort Collins, Colorado 80523. *Received June 15, 1983*

Abstract: Mixed-valence tri-μ-oxo iron acetates, $[Fe^{III}_2Fe^{II}O(OOCCH_3)_6L_3]$, L = H_2O or pyridine, are considered from the standpoint of their intramolecular electron transfer rates. Data from Mössbauer and infrared spectra and solution redox chemistry indicate that these complexes are in the Robin and Day class II, but with appreciable electron delocalization. Adiabatic potential energy surfaces are calculated for the three-center mixed-valence case and fitted to the physical data available for the mixed-valence iron trimers.

Although a great many mixed-valence compounds have been examined, it has been possible to get direct information on the dynamics of the intramolecular electron transfer process in only a few cases.[3-5] Of particular interest are the tri-μ-oxo iron acetates $[Fe^{III}_2Fe^{II}O(OOCCH_3)_6L_3]$, L = H_2O or pyridine. At low temperatures, the Mössbauer spectra[4,6] of these complexes reveal the existence of discrete Fe(III) and Fe(II) states, in the expected 2:1 ratio, thereby establishing valence trapping, or Robin and Day class II behavior.[7] At higher temperatures, a single Mössbauer absorption is seen, suggesting that the valencies have become equivalent by an electron transfer process, eq 1, i.e., Robin and

$$Fe^{III}Fe^{III}Fe^{II} \xrightarrow{k_{et}} Fe^{III}Fe^{II}Fe^{III} \quad (1)$$

Day class III behavior. There are two ways in which such equivalence can occur, one apparent and one real. The first is simply that the rate constant k_{et} has increased according to the Arrhenius law, eq 2, to the point where the rate is fast compared

$$k_{et} = \nu_0 \exp(-E_a/RT) \quad (2)$$

to the time frame of the experimental technique ($\approx 10^{-8}$ s in the case of the Mössbauer experiment). The second is that the molecular structure changes with temperature until the sites become structurally identical. In such a case the valencies are equivalent with respect to any experimental probe that has a time frame longer than that of a purely electronic transition ($\approx 10^{-14}$ s).

The Mossbauer data suggest that in the present complexes the latter type of transition does occur. The model used to fit the spectra as a function of temperature leaves not only the electron transfer relaxation time but also the isomer shifts and quadrupole splittings as adjustable parameters. As the temperature is increased, the isomer shifts and quadrupole splittings for Fe(III) and Fe(II) sites converge on each other. For the aquo complex, rough extrapolation suggests that they will converge between 300 and 350 K. For the pyridine complex the data are of poorer quality, but comparison with the aquo complex suggests that the convergence will be at a lower temperature.

Infrared data however indicate that the mixed-valence complexes are intermediate between localized and delocalized descriptions at lower temperatures as well. For a class III delocalized formulation the symmetry would be D_{3h} and the vibrational spectrum would be expected to correlate band for band with those of the fully oxidized complexes, $[Fe^{III}_3O(OOCCH_3)_6L_3]^+$. For a class II localized formulation the symmetry would be lowered to C_{2v} and the spectrum would correlate with those of mixed-metal complexes $[M_2M'O(OOCCH_3)_6L_3]^{n+}$. In the metal–carboxylate stretching region, the expected symmetry lowering was searched for but not found.[8b] Although the bands were broad and might therefore conceal some small splittings, the result suggested that in the mixed-valence complexes the difference between Fe(III) and Fe(II) is at least partly suppressed. More recent data provide clearer support for this. In the symmetrical Fe^{III}_3O complexes, the doubly degenerate asymmetric Fe_3O stretch has been identified[8a,9] (see Figure 1 and caption). In the mixed-metal series $Fe^{III}_2M'O$, M' = Mn, Co, Ni, the degeneracy of this mode is lifted and a doublet is seen. In the mixed-valence $Fe^{III}_2Fe^{II}O$ complexes the doublet is detectable, but in comparison with the mixed-metal complexes (and particularly in the pyridine series) the splitting is less and the component bands are broader and less intense.

(1) Presented in part at the Conference on Inorganic Reaction Mechanisms, Wayne State University, Detroit, MI, June 1981.
(2) (a) East Anglia; (b) Vermont; (c) deceased; (d) Colorado.
(3) Gagnê, R. R.; Koval, C. A.; Smith, T. J.; Cimolino, M. C. *J. Am. Chem. Soc.* **1979**, *101*, 4571.
(4) Dziobkowski, C. T.; Wrobleski, J. T.; Brown, D. B. *Inorg. Chem.* **1981**, *20*, 679.
(5) Sanchez, C.; Livage, J.; Launay, J. P.; Fournier, M.; Jeannin, J. *J. Am. Chem. Soc.* **1982**, *104*, 3194.
(6) Lupu, D.; Barb, D.; Filoti, G.; Morariu, M.; Tarnia, D. *J. Inorg. Nucl. Chem.* **1972**, *34*, 2803.
(7) Robin, M. B.; Day, P. *Adv. Inorg. Chem. Radiochem.* **1967**, *10*, 247.
(8) (a) Johnson, M. K.; Powell, D. B.; Cannon, R. D. *Spectrochim. Acta, Part A* **1981**, *37A*, 995; (b) *Ibid.* **1982**, *38A*, 307.
(9) Montri, L.; Cannon, R. D.; in preparation.

0002-7863/84/1506-2591$01.50/0

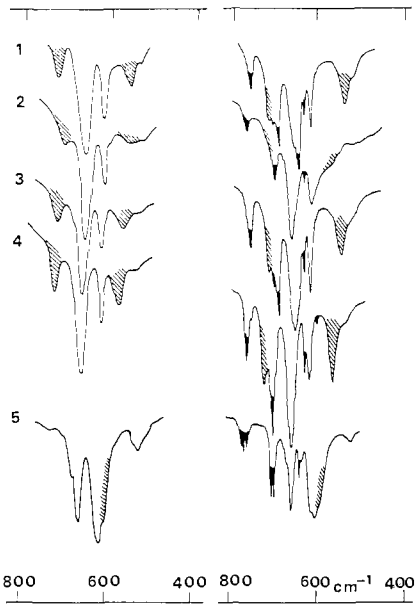

Figure 1. Infrared spectra (KBr disks, T = 300 K) of complexes $[Fe^{III}_2M'O(OOCCH_3)_6L_3]$, M′ = Mn, Fe, Co, Ni; and $[Fe^{III}_3O(OOCCH_3)_6L_3]^+$ (spectra 1–5); L = H_2O (left), L = pyridine (right). Unmarked bands are assigned to carboxyl vibrations δ(OCO), π(OCO), and ρ(OCO), on the basis of shifts upon deuteration of CH_3. Bands shaded black are assigned to pyridine ring vibrations (shifts upon deuteration of C_5H_5N). The hatched bands are assigned to the $Fe_2M'O$ and Fe_3O vibrations referred to in the text. They are shifted when central ^{16}O is replaced with ^{18}O.

Evidently the two oxidation states of Fe are distinguishable on the infrared time frame, but they are not so sharply distinct as if they were pure Fe(III) and Fe(II).

X-ray data, at room temperature, do not show any difference between the Fe sites.[10] This, however, is equally consistent with a class III structure or with a disordered structure of randomly oriented class II molecules. Indeed, in the mixed-metal complexes $[Fe^{III}_2M^{II}O(OOCCH_3)_6(py)_3]$, M = Mn, Co,[11] and $[Cr^{III}_2Fe^{III}O(OOCCH_3)(py)_3]^+$,[12] the metal sites are likewise indistinguishable.

For binuclear mixed-valence systems, there are well-known quantitative criteria for electron delocalization, which in principle make it possible to place a given system on a scale ranging from class I, with no interaction, to class III, with complete delocalization.[13-16] For a moderate interaction, the thermal activation energy E_a and intervalence charge transfer energy E_{op} are related by[15,17]

$$E_a = \tfrac{1}{4}E_{op} + \beta + \beta^2/E_{op} \quad (3)$$

where β is a coupling constant, while the ground-state resonance energy, defined as the difference between the actual energy of the complex and that for a hypothetical molecule with the same structure but no interaction, is given by[15]

$$E_{res} = \beta^2/E_{op} \quad (4)$$

The main assumptions underlying these results are that the framework vibrations are harmonic, that only one vibrational mode, of the appropriate symmetry type, is coupled to the electron transfer, that only one orbital from each metal atom is involved and that the usual first-order perturbation treatment can be applied, so that β is the resonance integral between the two orbitals.

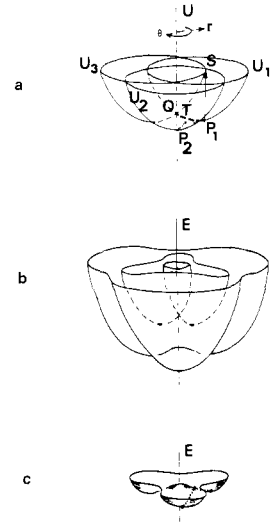

Figure 2. Energy surfaces for variation of the r and θ coordinates of the complex $(MX_6)_3$. (a) Zero-order, no interaction (cf. eq 7). The three paraboloids intersect at O. Points P_1, P_2 are at the minima of U_1, U_2. Point T is at the minimum of the intersection curve of U_1 and U_2. Point S is vertically above P_1, on the intersection curve of U_2 and U_3. (b) The first-order surfaces defined by eq 11 of the text, when $0 > c > -(^2/_3)$. (c) The E_1 surface, lowest part only. The broken curve P_1O in (a) is the energy curve for an E vibration of the complex. The dotted curves in (a) and (c) are reaction paths for thermal electron transfer.

In the present case, as shown below, all three energies, E_{op}, E_a, and E_{res}, are available, but the two-center model does not apply. For a quantitative comparison, we have developed a three-center model with the same assumptions.[18]

Neglecting differences between the ligands, we represent the trinuclear complex as three octahedral units $M^{(1)}X_6$, $M^{(2)}X_6$, $M^{(3)}X_6$, with atoms M at the points of an equilateral triangle. Considering only breathing vibrations of the three units, the total potential energy U is

$$U = \tfrac{1}{2}f(d_1 - d_1°)^2 + \tfrac{1}{2}f(d_2 - d_2°)^2 + \tfrac{1}{2}f(d_3 - d_3°)^2 \quad (5)$$

where d_1, d_2, and d_3 are the M–X bond distances, $d_1°$, etc. are the equilibrium values, and f is the force constant for the breathing mode, assumed to be the same for all three units. In the absence of coupling, we have three electronic configurations, with the electron localized at M atoms 1, 2, and 3, respectively, and energies U_1, U_2, U_3 given by eq 5 with $d_1°$, $d_2°$, $d_3°$ equal to d^{II}, d^{III}, d^{III}; d^{III}, d^{II}, d^{III}; d^{III}, d^{III}, d^{II} (where d^{II} and d^{III} are the equilibrium M–X distances in pure $Fe^{II}X_6$ and $Fe^{III}X_6$ configurations). Introducing coordinates $p = d_1 + d_2 + d_3$, $q_1 = d_1 - {}^1/_2d_2 - {}^1/_2d_3$, $q_2 = -{}^1/_2d_1 + d_2 - {}^1/_2d_3$, $q_3 = -{}^1/_2d_1 - {}^1/_2d_2 + d_3$, $p° = d_1° + d_2° + d_3°$, etc., the energies of the three configurations are

$$U_i = (f/6)(p - p°)^2 + (2f/9)[q_1^2 + q_2^2 + q_3^2 + \tfrac{3}{2}a^2 - 3aq_i] \quad (6)$$

(10) New, D. B., Ph.D. Thesis, Queen Mary College, London, 1975.
(11) Blake, A. B.; Yavari, A.; Kubicki, H. *J. Chem. Soc., Chem. Commun.* **1981**, 796.
(12) Kowiak, T.; Kubiak, M.; Szymanska-Buzar, T.; Jezowska-Trzebiatowska, B. *Acta Crystallogr., Sect B* **1977**, *B33*, 3106.
(13) Hush, N. S. *Prog. Inorg. Chem.* **1967**, *8*, 391.
(14) Mayoh, B.; Day, P. *J. Am. Chem. Soc.* **1972**, *94*, 2885.
(15) Cannon, R. D.; "Electron Transfer Reactions"; Butterworth: London, 1980; p 274.
(16) Schatz, P. N. In "Mixed Valence Compounds"; Brown, D. B., Ed.; Reidel: New York, 1980; pp 115–150.
(17) Throughout this paper β values are regarded as negative, i.e., the opposite sign to β of ref 15.
(18) While this work was in progress, Launay and Babonneau published a model for trinuclear mixed-valence systems, with particular reference to heteropolymolybdates (ref 19; cf. ref 20). They use the same physical concepts and come to essentially similar theoretical conclusions. In addition they discuss the case $c > 0$. Launay and Babboneau's calculations are based on computer-plotted contour diagrams of the energy surfaces, whereas we have used the explicitly solved eq 10–12. For comparison between the two treatments, Launay and Babboneau's parameters k, l, W_s, and B correspond to our f, af, β, and $c/3$. Discrepancies between the two treatments are minor: see note 22. See also: Borsch, S. A.; Kotov, I. N.; Bersuker, I. B. *Chem. Phys. Lett.* **1982**, *89*, 381.
(19) Launay, J. P. and Babonneau, F., *Chem. Phys.*, **1982**, *67*, 295.
(20) Sanchez, C.; Livage, J.; Launay, J. P.; Fournier, M.; Jeannin, Y. *J. Am. Chem. Soc.* **1982**, *104*, 3194.
(21) Substituting i = 1 in these equations gives E_2 when $x > 0$, E_3 when $x < 0$; i = 2 gives E_1 for all x; i = 3 gives E_3 when $x > 0$, E_2 when $x < 0$.

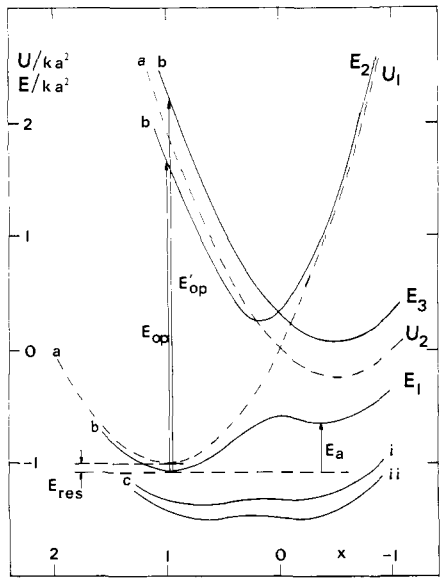

Figure 3. Cross sections of energy surfaces in the plane $\theta = 0$. (a) The zero-order surfaces, eq 8 and 9. (b) The first-order surfaces given by eq 12 and 13, when $c = -0.3$. (c) The E_1 surface for particular values of c: (i) $c = -{}^2/_3$; (ii) $c = -{}^3/_4$.

where $a = d^{II} - d^{III}$ and $i = 1, 2, 3$. More conveniently these may be written

$$U_i = (k/2)(p - p^\circ)^2 + ka^2 + k[r^2 - 2ar\cos(\theta - 2\pi(i-1)/3)] \quad (7)$$

where we have used $q_i = r\cos(\theta - 2\pi(i-1)/3)$, $k = f/3$. Assuming that only variations in r and θ are coupled to electron transfer, we drop the first two terms in eq 7. Plots of U_1, U_2, and U_3 against r and θ are shown in Figure 2a. A complex in its ground state with the electron localized at $M^{(1)}$ is represented by the point P_1 at the bottom of the surface U_1. Intervalence charge transfer is represented by the vertical transition to S, which is on the intersection curve of U_2 and U_3. Thermal electron transfer from $M^{(1)}$ to $M^{(2)}$ is represented by the lowest-energy path from P_1 to P_2, crossing the point T that is at the bottom of the intersection curve of U_1 and U_2. A section through the surfaces, in the vertical plane $\theta = 0$, is shown in Figure 3, curves designated with an a. The parabolas have the equations

$$U_1 = ka^2(x^2 - 2x) \quad (8)$$

$$U_2 = U_3 = ka^2(x^2 + x) \quad (9)$$

where $x = r/a$. They intersect at $x = 0$, $U = 0$, and the minima are at $x = 1$, $U_1 = -ka^2$, and $x = -{}^1/_2$, $U_2 = U_3 = -{}^1/_4ka^2$. The intervalence transfer energy is given by $(U_2 - U_1)$ when $r = a$, i.e., $E_{op} = 3ka^2$, while the thermal activation energy is the difference of the two minima, $E_a = {}^3/_4ka^2$. Thus "Hush's law", $E_a = {}^1/_4E_{op}$ when there is no interaction,[13] applies to the three-center as well as to the two-center model.

To introduce coupling we define the integrals $H_{ij} = \int \phi_i H \phi_j \, d\tau$ and write $H_{ij} = \beta$ when $i \neq j$, $H_{ij} = U_i$ when $i = j$. With the neglect of overlap, the secular equation is

$$\begin{vmatrix} U_1 - E & \beta & \beta \\ \beta & U_2 - E & \beta \\ \beta & \beta & U_3 - E \end{vmatrix} = 0 \quad (10)$$

The three solutions for E are given by[21]

$$E_i = k\{r^2 + 2a(r^2 + a^2c^2)^{1/2}\cos(\psi/3 + 2\pi(i-1))/3\} \quad (11a)$$

$$\psi = \cos^{-1}\{(-r^3\cos 3\theta + a^3c^3)/(r^2 + a^2c^2)^{3/2}\} \quad (11b)$$

where $c = \beta/ka^2$. When plotted against r and θ, they give the surfaces shown in Figure 2b. The upper surface has a nodal point at $r = 0$. The energies at $r = 0$ are 2β, $-\beta$, $-\beta$ (β being negative[17]),

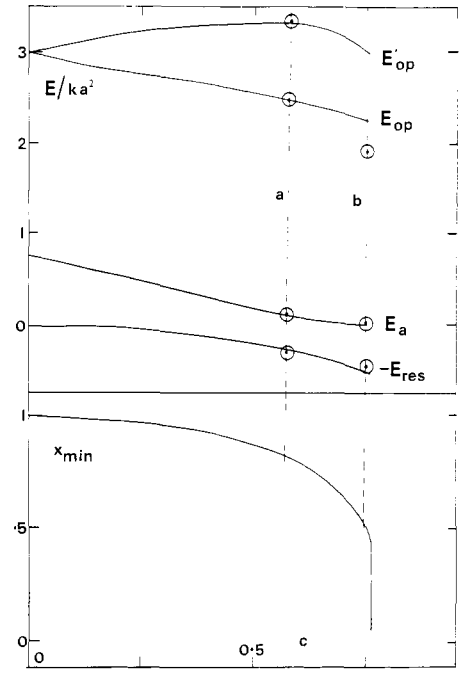

Figure 4. Variation of energy parameters, and of x_{min} with c. Experimental energies for $[Fe_3O(OOCCH_3)_6L_3]$ are fitted to the curves (a) L = H_2O; (b) L = py.

and this corresponds to D_{3h} symmetry with a single ground state and a doubly degenerate excited state. Cross sections in the $\theta = 0$ plane are shown in Figure 3, curves b and c. They are given by

$$E_{1,2} = ka^2\{x^2 - {}^1/_2x + {}^1/_2c \pm {}^1/_2(9x^2 + 6cx + 9c^2)^{1/2}\} \quad (12)$$

$$E_3 = ka^2(x^2 + x - c) \quad (13)$$

For small c, the lowest surface has three energy wells and a central hump. The minimum-energy paths between the wells do not pass over the hump, however, but through three separate saddle points (Figure 2c). With increasingly negative c, the hump is reduced until it disappears at $c = -{}^2/_3$. Three wells are still present, but they are very shallow, and the minimum energy paths now pass through the center. With more negative c, a fourth very shallow depression appears at the center. At $c = -{}^3/_4$, all four wells are the same depth, and finally at $c = -0.7611$,[22] only the single central energy well remains. The transition from class II to class III may be said to occur at $c = -{}^3/_4$. When c is small, the value of E_1 at the lower minimum is hardly different from U_1, but at the saddle point (the upper minimum in Figure 3) it is significantly lowered, by approximately $-\beta$, because of delocalization of the electron between the equivalent sites $M^{(2)}$ and $M^{(3)}$. For the same reason, there are *two* intervalence charge-transfer energies, marked E_{op} and E'_{op} in Figure 3. The value of x at the lower minimum (x_{min}) measures the ground-state distortion of the structure. For a structure with bond lengths corresponding to pure oxidation states Fe(II) and Fe(III), $x_{min} = 1$. With increased delocalization, x_{min} decreases, gradually at first, until $c = -0.7611$, whereupon x_{min} falls abruptly from 0.378 to 0, and the structure changes from C_{2v} to D_{3h}. Plots of E'_{op}, E_{op}, E_a, and E_{res}, and of x_{min}, against c are shown in Figure 4. The test of the model is how well the experimental energies can be fitted to these curves, and the measure of delocalization is the value of c, or β, required to give the best fit.

Experimental energies are listed in Table I. Values of E_a are from the Mössbauer data. Values of E_{op} are from reflectance

(22) This value was obtained by numerical methods, as one of the three values of c for which the curve $E_1(x)$ has a horizontal inflection (i.e., $dE_1/dx = d^2E_1/dx^2 = 0$), the other values being $c = -{}^2/_3$, $x = 0$; $c = -{}^3/_4$, $x = -{}^1/_4$. Our value −0.7611 differs from that of Launay and Babonneau,[19] who proposed −0.75.

Table I. Energy Parameters for the Complexes $[Fe_3O(OOCCH_3)_6L_3]^a$

L	py	H_2O
E_{op}	7.0[b]	9.1[e]
E_a	0.26 ± 0.021[c]	0.60 ± 0.32[c]
E_{res}	1.99[d]	1.15[f]

[a] Table entries are E/Lhc^{-1}; units are 10^3 cm^{-1}. [b] Reference 23. Broad band with peak at 7400 cm^{-1} and shoulder ca. 6000 cm^{-1}. [c] From linear least-squares fitting to plots of log k_{et} against T^{-1} (data of ref 4), in the range T = 50–300 K. [d] From data cited in the text and eq 14. [e] Reference 4, Figure 10. Broad band, with peaks at ca. 8400 and 9700 cm^{-1}. [f] From polarographic reduction potentials of $[Cr_2FeO(OOCCH_3)_6(OH_2)_3]^+$ and $[Fe_3O(OOCCH_3)_6(OH_2)_3]^+$, $E_{1/2}$ = −0.200 and −0.030 V vs. SCE, 25 °C, 4 M HOAc. Quasi-reversible waves with similar heights and midpoint slopes (ref 25).

spectra of the solids. For the aquo complex, a band at 13 800 cm^{-1} was previously suggested as the lowest intervalence charge transfer,[4] but Blake et al. have since reported spectra of a number of mixed-metal and mixed-valence complexes in the pyridine series[23] and they assign a broad band at ca. 7000 cm^{-1} as the lowest intervalence charge transfer. Two other bands at 13 000 and 17 000 cm^{-1} are tentatively ascribed to charge transfer with excitation of the receptor sites. We have reassigned the spectrum of the aquo complex accordingly.

Values of E_{res} are estimated from electrochemical data in solution. The complex $[Cr_3O(OOCCH_3)_6(py)_3]^+$ is electrochemically inactive, but in pyridine solution the Cr_2FeO and Fe_3O analogues are reduced reversibly with $E_{1/2}$ = −0.38 and −0.104 V vs. SCE.[24] These data when combined give the equilibrium

$$[Cr_2Fe^{II}O(OOCCH_3)_6(py)_3] + [Fe^{III}_3O(OOCCH_3)_6(py)_3]^+ \overset{K}{\rightleftharpoons} [Cr_2Fe^{III}O(OOCCH_3)_6(py)_3]^+ + [Fe^{III}_2Fe^{II}O(OOCCH_3)_6(py)_3] \quad (14)$$

with $K = 4.8 \times 10^4$, at 25 °C. Because the electron involved in the reduction of the triiron complex has equal probability of attaching to any Fe site, the equilibrium is favored by a statistical factor of 3. After discounting this, we estimate the resonance stabilization of the mixed-valence complex as $E_{res} = 2.3RT \log (K/3)$ = 5.7 kcal mol^{-1}. This argument assumes (1) that solvation energies of the four species in eq 13 cancel and (2) that the replacement of Fe by Cr in the trinuclear structure does not distort the ligand framework so much as to change significantly the $E_{1/2}$ values, or rather that any such changes also cancel. For the aquo complexes, $E_{1/2}$ values from polarography in aqueous media have been used.[25] These are quasi-reversible and therefore require the additional assumption that electrode kinetic factors are similar for the two couples. The values of $E_{1/2}$ for the aquo complexes are regarded as provisional.

The experimental energies are entered in Figure 4. They were fitted to the curves by choosing the value of c that gave the ratios of the energies in best agreement with experiment. Thus for either complex, c and ka^2 were treated as adjustable parameters. For the aquo complex, a good fit is obtained with $c = \beta/ka^2 = -0.57$ and ka^2 = 10.4 kcal mol^{-1} (3640 cm^{-1}). Moreover the previously reported spectral band at 13 800 cm^{-1} agrees well with the predicted E'_{op}. For the pyridine complex, the fit is fairly satisfactory, with c just above −0.75, and ka^2 almost the same as before, 10.5 kcal mol^{-1} (3680 cm^{-1}).

In the simplified model used here, r is the normal coordinate for a combination of the (MX_6) breathing vibrations. (This is the E component of $\nu(MX_6)_3$ if the symmetry is taken to be D_{3h}, or the A_1 component of $\nu((M'X_6)(MX_6)_2)$ in the lowered symmetry of C_{2v}). Any other vibration of the same symmetry type could be used, and in the actual complexes, vibrations expected to couple with electron transfer include $\nu_{as}(OFe_3)$ and the appropriate combinations of $\nu_s(FeO_4)$ and of ν(Fe–N). Coupling between these vibrations must also be envisaged (this aspect is now being studied), and the effective reaction coordinate should include all of them. Until coupling effects have been worked out, further discussion is withheld, except to note that the vibrational quanta are in the range 200–600 cm^{-1}, which is greater than or equal to the activation energies. It seems likely that in the pyridine complex, the lowest vibrational level is delocalized, though still biased toward the C_{2v} geometry, while in the aquo complex, the vibrational ground state may be below the barrier, and the first vibrationally excited state above it.

Meanwhile, though the model is oversimplified, all the data are consistent with the conclusion that these trinuclear iron acetates are valence-trapped at room temperature, but with appreciable electron delocalization, and that the pyridine complex is particularly close to the Robin and Day class II/class III borderline.

Acknowledgment. Support by the Department of Energy, Office of Basic Sciences (DE-AC02 80ER10589), is gratefully acknowledged (C.M.E.). We thank Dr. A. B. Blake for samples of mixed-metal complexes and Drs. M. B. Hursthouse and P. Thornton for useful discussions and for unpublished data. L.M. holds a University of East Anglia Overseas Studentship.

Registry No. $Fe^{III}_2Fe^{II}O(OOCCH_3)_6(H_2O)_3$, 36354-69-5; $Fe^{III}_2Fe^{II}O(OOCCH_3)_6(py)_3$, 35268-77-0.

(23) Blake, A. B.; Yavari, A. *J. Chem. Soc., Chem. Commun.* **1982**, 1247.
(24) Pt electrodes, $(n\text{-Bu})_4ClO_4$ electrolyte, 25 °C: Marshall, K. M.; Brown, D. B.; Elliott, C. M., unpublished results.
(25) Johnson, M. K. Ph.D. Thesis, University of East Anglia, 1977.
(26) Montri, L., experiments in progress.